

# SPICEprop: Backpropagating Errors Through Memristive Spiking Neural Networks

Peng Zhou, *Student Member, IEEE*, Jason K. Eshraghian, *Member, IEEE*,  
Dong-Uk Choi, and Sung-Mo Kang, *Life Fellow, IEEE*

**Abstract**—We present a fully memristive spiking neural network (MSNN) consisting of novel memristive neurons trained using the backpropagation through time (BPTT) learning rule. Gradient descent is applied directly to the memristive integrate-and-fire (MIF) neuron designed using analog SPICE circuit models, which generates distinct depolarization, hyperpolarization, and repolarization voltage waveforms. Synaptic weights are trained by BPTT using the membrane potential of the MIF neuron model and can be processed on memristive crossbars. The natural spiking dynamics of the MIF neuron model are fully differentiable, eliminating the need for gradient approximations that are prevalent in the spiking neural network literature. Despite the added complexity of training directly on SPICE circuit models, we achieve 97.58% accuracy on the MNIST testing dataset and 75.26% on the Fashion-MNIST testing dataset, the highest accuracies among all fully MSNNs.

**Index Terms**—Neuromorphic computing, memristor, spiking neural network, supervised learning, backpropagation.

## I. INTRODUCTION

**S**PIKING Neural Networks (SNNs), often referred to as the third generation of neural networks, draw inspiration from biological neurons to enable heightened efficiency over conventional neural networks. When processed on neuromorphic hardware, SNNs have shown significant energy and latency savings due to their activation sparsity, spike-based representations of data, and event-based data processing [1]–[4]. Recently, the remarkable success of backpropagation in the training of Deep Neural Networks (DNNs) has broadened and inspired research on SNNs. By unrolling the computational graph of spiking neuron models, SNNs can take advantage of the backpropagation through time (BPTT) algorithm [5] such that a global error is calculated in the final layer and backpropagated across the full history of the SNN dynamics. By analogy, we propose that circuit-level neuron models described by dynamical state equations can also be trained in a similar manner. In doing so, the rich dynamics of nonlinear circuit elements, such as memristors, can be fully leveraged during the network optimization process.

The memristor, theoretically postulated by Chua in 1971 [6] and generalized by Chua and Kang in 1976 [7], has become a commercially available technology that can be integrated in the back-end-of-the-line (BEOL) of modern CMOS processes [8], [9]. The non-volatile retention capacity of the memristor is

often likened to synaptic memory [10]–[13], and its threshold-switching characteristics have been exploited in spiking neuron models [14]–[17]. However, much of the prior work on memristive spiking neural networks (MSNNs) is constrained to using either memristive synapses *or* memristive neurons, but not both. Memristive synaptic arrays are used only for non-volatile memory retention, where networks are trained offline and thus, do not harness the complex dynamics of memristors. Networks of memristive neurons (‘neuristors’), on the other hand, are challenging to train and only used in small-scale networks constrained to simple tasks, such as low-dimensional pattern recognition solved via associative or local learning rules. The work in [18] successfully integrates a fully memristive network, including memristive synapses and neurons, to perform basic pattern recognition, but the memristors used in this work are not accessible to the broader research community. The work presented in [19] uses analog ReLU activations with memristive synapses to achieve 93.63% testing accuracy on the MNIST dataset. As a non-spiking network, analog signals are noise prone, whereas spikes are error tolerant discrete events distributed in time.

In this paper, we scale up the complexity of learnable tasks in fully memristive SNNs by directly applying gradient descent to the nonlinear state evolution of memristive neurons and synapses. Both neurons and synapses are modeled using memristors. The memristive integrate-and-fire (MIF) neuron model is designed to achieve distinct depolarization, hyperpolarization, and repolarization voltage phases with a minimal set of circuit elements. Memristive synapses interconnect layers of neurons. To train the fully memristive network, we propose SPICEprop, an application of error backpropagation to large-scale networks derived from SPICE circuit models. This enables dynamical, time-varying memristive neurons to achieve much higher accuracy on data-driven tasks than has been previously reported with MSNNs. By relying on the analog spiking characteristics that naturally occur in the MIF neuron model, the non-differentiability of spike-based activations are completely avoided. This means SPICEprop does not rely on surrogate gradient techniques that are commonly used to train SNNs, which calculates biased gradient estimators to circumvent the dead neuron problem [20]. To promote broad accessibility of our methods, we use SPICE models of commercially available, low-cost memristors to demonstrate the efficacy of SPICEprop in a supervised deep learning framework.

P. Zhou, D. Choi, and S. M. Kang are with the Department of Electrical and Computer Engineering, UC, Santa Cruz, CA, USA.

J. K. Eshraghian is with the Dept. of Electrical Engineering and Computer Science, University of Michigan, Ann Arbor, MI, USA.

## II. METHODS

### A. MIF model

Our MSNN adopts the MIF neuron model shown in Fig. 1 [21]. The MIF neuron is characterized by the differential equations below:

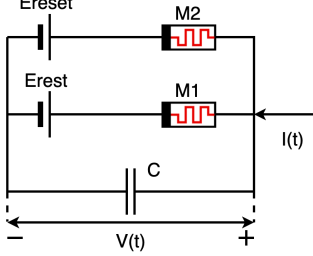


Fig. 1. A memristive integrate-and-fire (MIF) neuron consists of two memristors  $M_1$  and  $M_2$ , connected to DC voltage sources  $E_{rest}$  and  $E_{reset}$ , in parallel with a capacitor  $C$ . The MIF neuron is provably minimal in generating a membrane potential traversing from a rest voltage level to a threshold voltage level, then to a reset voltage level, and then back to the rest potential when a current pulse is applied.

$$\frac{dv}{dt} = \frac{I - G_1(v - E_{rest}) - G_2(v - E_{reset})}{C} \quad (1a)$$

$$\frac{dx_1}{dt} = \frac{1}{\tau_1} \left( \frac{1 - x_1}{1 + e^{\frac{v_{on1} - (v - E_{rest})}{k_{th}}}} - \frac{x_1}{1 + e^{\frac{(v - E_{rest}) - v_{off1}}{k_{th}}}} \right) \quad (1b)$$

$$\frac{dx_2}{dt} = \frac{1}{\tau_2} \left( \frac{1 - x_2}{1 + e^{\frac{v_{on2} - (v - E_{reset})}{k_{th}}}} - \frac{x_2}{1 + e^{\frac{(v - E_{reset}) - v_{off2}}{k_{th}}}} \right) \quad (1c)$$

$$G_1 = \frac{x_1}{R_{on1}} + \frac{1 - x_1}{R_{off1}} \quad (1d)$$

$$G_2 = \frac{x_2}{R_{on2}} + \frac{1 - x_2}{R_{off2}} \quad (1e)$$

where  $G_1$  and  $G_2$  are the memductances,  $x_1$  and  $x_2$  are a pair of internal states,  $\tau_1$  and  $\tau_2$  are time constants governing the rate of change in internal states, and  $k_{th}$  is the effective thermal voltage. They are the characteristic variables of  $M_1$  and  $M_2$ , respectively. This system of equations mirrors several prominent SPICE memristor models, and has been used to emulate the commercially available KNOWM<sup>TM</sup> memristor.

For a physically plausible system, discrete spikes must be represented as continuous current inputs. An input spike train of Dirac delta pulses  $\sum_n \delta(t - t_j^n)$  is used to generate an alpha-shaped input current  $I$ , modeled by Eq. (2):

$$\tau_{syn} \frac{dI}{dt} = a - I \quad (2a)$$

$$\tau_{syn} \frac{da}{dt} = -a + W_i \cdot \sum_n \delta(t - t_i^n) \quad (2b)$$

where  $a$  is an internal state variable,  $\tau_{syn}$  is a time constant governing the shape of the alpha current,  $W_i$  is the synaptic weight between presynaptic neuron  $i$  and associated postsynaptic neuron.

The parameters used in this network are listed in Table I.

TABLE I  
MIF CIRCUIT PARAMETERS

Parameter	Value	Parameter	Value
$E_{rest}$	0 mV	$E_{reset}$	50 mV
$C$	100 pF	$k_{th}$	15 mV
$v_{off1}, v_{off2}$	5 mV	$v_{on1}, v_{on2}$	110 mV
$R_{off1}, R_{off2}$	0.1 M $\Omega$	$R_{on1}, R_{on2}$	1 k $\Omega$
$\tau_1, \tau_2$	100 steps	$\tau_{syn}$	100 steps

### B. Numerical Integration of MIF Model

The SPICE model of the memristor used in the MIF neuron described in Eq. (1) must be adapted to a recurrent form to be compatible in a deep learning framework. SPICE simulators employ a variety of ordinary differential equation (ODE) solvers, which, in the first order, are often equivalent to the backward Euler method. For compatibility with BPTT, we adopt the forward Euler method to find an approximate solution to the MIF network, as the forward Euler method provides an explicit update equation. As such, we retain the temporal dynamics of the MIF neuron, and also derive a discrete time representation of the MIF neuron that can be unrolled across time steps for use with the BPTT algorithm. The approximate solution of a MIF neuron model with alpha current dynamics using the forward Euler method is provided in Eq. (3).

$$a[t+1] = -\frac{a[t]}{\tau_{syn}} + a[t] + \sum_j W_j \cdot S_j \quad (3a)$$

$$I[t+1] = \frac{a[t] - I[t]}{\tau_{syn}} + I[t] \quad (3b)$$

$$x_1[t+1] = \frac{1}{\tau_1} \left( \frac{1 - x_1[t]}{1 + e^{\frac{v_{on1} - (v[t] - E_{rest})}{k_{th}}}} - \frac{x_1[t]}{1 + e^{\frac{(v[t] - E_{rest}) - v_{off1}}{k_{th}}}} \right) + x_1[t] \quad (3c)$$

$$x_2[t+1] = \frac{1}{\tau_2} \left( \frac{1 - x_2[t]}{1 + e^{\frac{v_{on2} - (v[t] - E_{reset})}{k_{th}}}} - \frac{x_2[t]}{1 + e^{\frac{(v[t] - E_{reset}) - v_{off2}}{k_{th}}}} \right) + x_2[t] \quad (3d)$$

$$G_1[t+1] = \frac{x_1[t+1]}{R_{on1}} + \frac{1 - x_1[t+1]}{R_{off1}} \quad (3e)$$

$$G_2[t+1] = \frac{x_2[t+1]}{R_{on2}} + \frac{1 - x_2[t+1]}{R_{off2}} \quad (3f)$$

$$v[t+1] = \frac{I[t] - G_1[t](v[t] - E_{rest}) - G_2[t](v[t] - E_{reset})}{C} + v[t] \quad (3g)$$

Fig. 2 shows the simulation results across 1,000 time steps. Each time step is of duration 0.01 ms and the total time simulated is 10 ms. The rest, integrate, threshold, and reset

performances are correctly simulated by a SPICE simulator to match the dynamics of the alpha synapse current and the MIF neuron modeled by the ODEs in Eq. (1) and (2).

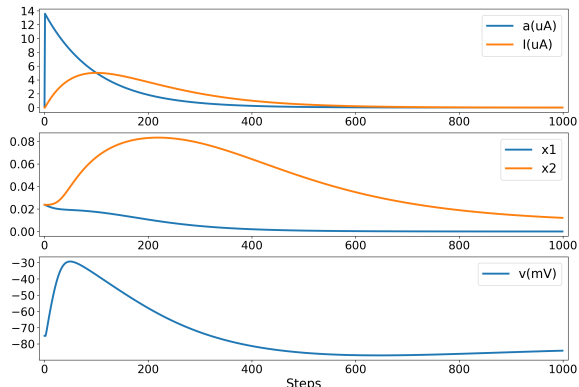


Fig. 2. Simulation results of MIF neuron solved using forward Euler numerical integration. The results matches the quantitative dynamics of solved by a SPICE simulator. Top: Alpha synaptic current dynamics. Middle: Internal states  $x_1, x_2$ . Bottom: Voltage response  $v$ .

### C. Backpropagation Through Time in Memristive Spiking Neural Networks

The discrete-time solution in Eq. (3) is illustrated as an MSNN computational graph in Fig. 3, resembling an unrolled recurrent neural network. The loss can be calculated based on either spiking activity or the membrane potential. Two observations support the use of the membrane potential. Firstly, an increase in potential of the correct output neuron drives the neuron to spike, while decreasing the potential of the incorrect neuron classes makes these neurons silent. Applying the target to the membrane potential can serve as a proxy for modulating the spiking behavior. Secondly, the MIF membrane potential is autonomously reset after a spike is elicited without the need for extra circuitry; i.e., the spike is part of the membrane potential waveform which is weighted and propagated to downstream layers. Therefore, a fully analog MSNN can be trained without reliance on additional surrogate gradient calculation steps, as used in almost all multi-layer SNNs trained via error backpropagation [1], [20].

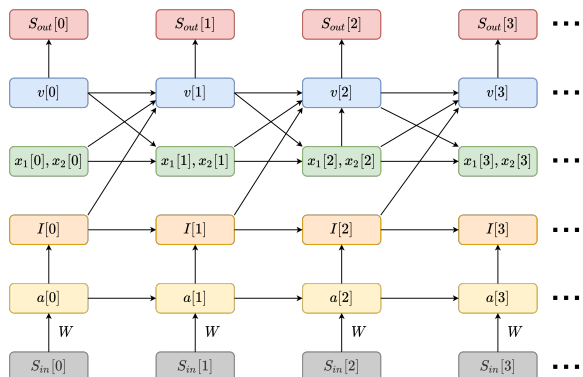


Fig. 3. Unrolled MSNN computational graph in discrete time.

### D. Network Architecture

To validate the use of MIF neurons in a deep learning framework, we used a 4-layer neural network shown in Fig. 4. In the input layer, there are  $28 \times 28 = 784$  input units. The first hidden layer consists of 100 neurons followed by a ReLU activation, and the second hidden layer contains 10 neurons followed by a ReLU activation. Finally, the output layer consists of 10 MIF neurons. Fully connected (all-to-all) weights are used between each layer.

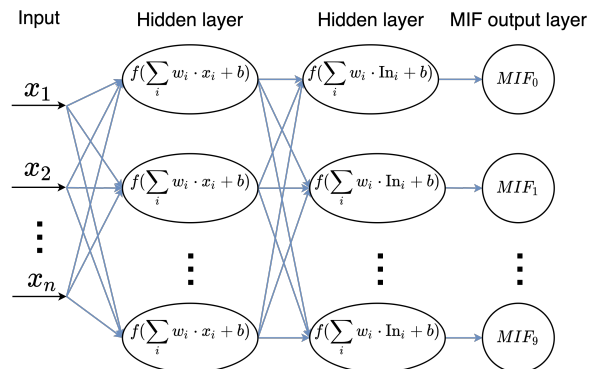


Fig. 4. The MSNN architecture.

## III. RESULTS

The automatic differentiation engine from PyTorch v1.10.1 was used to perform BPTT through the network in Python 3.8. For training and testing, we used the MNIST dataset [22] which consists of 70,000 samples of handwritten digits. During the training process, 1,000 time steps are simulated for each input image sample. Over the 1,000 steps, the input pixel intensity is fed to the network only at steps 0, 400, and 800 to promote sparse network activity. The negative log-likelihood loss is applied to the membrane potential, i.e.,  $v(t)$  in the MIF circuit in Fig. 1, at each time step. In other words, the goal of the network is to maximize the voltage across the MSNN circuit of the correct class. The total loss is summed prior to backpropagating the error through the SPICE memristor model. The Adam optimizer is utilized as it performs well on both recurrent networks and stochastic problems [23]. For the Adam optimizer, the learning rate is set to  $10^{-4}$ , the initial decay rates for first and second order moments are set to  $\beta_1 = 0.9$ ,  $\beta_2 = 0.999$ . The learnable weights of dense layers are initialized by sampling from a uniform distribution  $U(-\sqrt{k}, \sqrt{k})$ , where  $k = \frac{1}{N_i}$  and  $N_i$  is the number of input features to layer  $i$ . The MSNN is trained for 40 epochs using a batch size of 200 samples. Accuracy is evaluated at every 10 training iterations. For the MNIST dataset, the training and testing accuracies across multiple epochs are shown in Fig. 5. 97.58% accuracy is achieved for the total MNIST test set. For a more challenging task using real-world data, we also train our MSNN on the Fashion-MNIST dataset, where we obtain 75.26% testing accuracy. This demonstrates the first functional result on the Fashion-MNIST dataset using analog MSNNs, and highlights the potential for MSNNs to be capable of moving beyond simple MNIST classification.

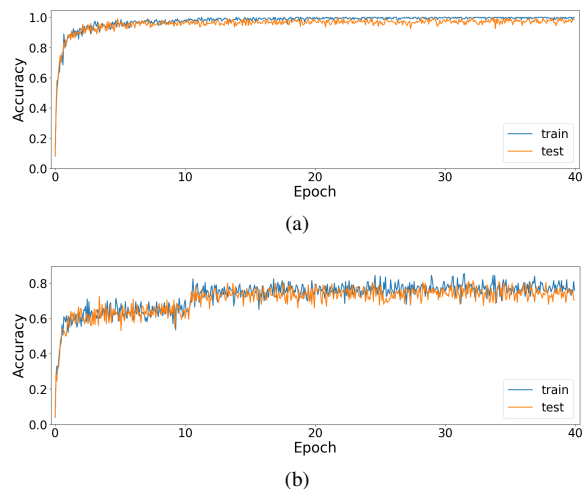


Fig. 5. Accuracy across epochs for training and testing processes for (a) MNIST dataset (b) Fashion-MNIST dataset.

#### IV. DISCUSSION AND CONCLUSION

We have confirmed the compatibility of circuit-level MSNNs with error-driven supervised learning. Our primary results show that MIF neurons based on SPICE models can be trained in a multi-layer neural network using BPTT, sidestepping the need for surrogate gradient signals. To the best of our knowledge, this is the first work to perform gradient descent directly on a network of SPICE models of memristive neurons that emit analog spikes.

While MSNNs are extremely power efficient, they are also highly challenging to train. We achieve state of the art accuracy on MNIST and Fashion-MNIST datasets when compared to all other networks of spiking MSNNs. Prior attempts on the MNIST dataset using memristive spiking neurons with error-driven optimization [24] only achieved 83.24%. The approach in [24] aims to fit memristive neurons to LIF neuron models, whereas our approach directly relies on the gradient of the naturally arising memristive dynamics during training, in order to achieve the accuracy boost to 97.58%.

Although SNNs add more latency for training due to the additional temporal dimension, there are many reasons why this approach is valuable and holds great potential:

- SNNs can exploit sparse data connections and activations to reduce memory access frequency, which we exploit by only presenting input data for 3 out of the total 1,000 time steps of simulation. [17], [25]–[27].
- A large-scale neural network based on the MIF neuron has a much higher density compared with the conventional CMOS counterparts by taking advantage of vertical BEOL CMOS integration.
- Area and power can be saved as less peripheral circuits are needed by eliminating the need for analog-to-digital converters (ADCs) and digital-to-analog converters (DACs) in bit-line current summation approaches; i.e., all spiking is a result of the natural evolution of the memristor’s state dynamics.
- The natural temporal dynamics of the MIF model allow for differentiable spike propagation through a MSNN,

eliminating the need for biased gradient estimators such as surrogate gradients.

Future work will involve further increasing the complexity of the datasets, accounting for the non-idealities present in memristive synapses, and stochasticity that is not designed in the SPICE model yet.

#### REFERENCES

- [1] J. K. Eshraghian, M. Ward, E. Neftci, X. Wang, G. Lenz, G. Dwivedi, M. Bennamoun, D. S. Jeong, and W. D. Lu, “Training spiking neural networks using lessons from deep learning,” *arXiv preprint arXiv:2109.12894*, 2021.
- [2] M. R. Azghadi, C. Lammie, J. K. Eshraghian, M. Payvand, E. Donati, B. Linares-Barranco, and G. Indiveri, “Hardware implementation of deep network accelerators towards healthcare and biomedical applications,” *IEEE Transactions on Biomedical Circuits and Systems*, vol. 14, no. 6, pp. 1138–1159, 2020.
- [3] P. Zhou, D.-U. Choi, J. K. Eshraghian, and S.-M. Kang, “A fully memristive spiking neural network with unsupervised learning,” *arXiv preprint arXiv:2203.01416*, 2022.
- [4] P. Zhou and S. Abbaszadeh, “Towards real-time machine learning for anomaly detection,” in *2020 IEEE Nuclear Science Symposium and Medical Imaging Conference (NSSMIC)*. IEEE, pp. 1–3.
- [5] P. J. Werbos, “Backpropagation through time: what it does and how to do it,” *Proceedings of the IEEE*, vol. 78, no. 10, pp. 1550–1560, 1990.
- [6] L. O. Chua, “Memristor—the missing circuit element,” *IEEE Transactions on Circuit Theory*, vol. 18, no. 5, pp. 507–519, 1971.
- [7] L. O. Chua and S. M. Kang, “Memristive devices and systems,” *Proceedings of the IEEE*, vol. 64, no. 2, pp. 209–223, 1976.
- [8] “eflash,” <https://www.tsmc.com/english/dedicatedFoundry/technology/specialty/eflash>.
- [9] “Mad200,” <https://mycmp.fr/nvm-mad200/>.
- [10] S. H. Jo, T. Chang, I. Ebong, B. B. Bhadviya, P. Mazumder, and W. Lu, “Nanoscale memristor device as synapse in neuromorphic systems,” *Nano letters*, vol. 10, no. 4, pp. 1297–1301, 2010.
- [11] M. Rahimi Azghadi, Y.-C. Chen, J. K. Eshraghian, J. Chen, C.-Y. Lin, A. Amirsoleimani, A. Mehonic, A. J. Kenyon, B. Fowler, J. C. Lee *et al.*, “Complementary metal-oxide semiconductor and memristive hardware for neuromorphic computing,” *Advanced Intelligent Systems*, vol. 2, no. 5, p. 1900189, 2020.
- [12] F. Cai, J. M. Correll, S. H. Lee, Y. Lim, V. Bothra, Z. Zhang, M. P. Flynn, and W. D. Lu, “A fully integrated reprogrammable memristor–cmos system for efficient multiply–accumulate operations,” *Nature Electronics*, vol. 2, no. 7, pp. 290–299, 2019.
- [13] T. Serrano-Gotarredona, T. Masquelier, T. Prodromakis, G. Indiveri, and B. Linares-Barranco, “Stdp and stdp variations with memristors for spiking neuromorphic learning systems,” *Frontiers in neuroscience*, vol. 7, p. 2, 2013.
- [14] M. D. Pickett, G. Medeiros-Ribeiro, and R. S. Williams, “A scalable neuristor built with mott memristors,” *Nature materials*, vol. 12, no. 2, pp. 114–117, 2013.
- [15] J. K. Eshraghian, K. Cho, C. Zheng, M. Nam, H. H.-C. Iu, W. Lei, and K. Eshraghian, “Neuromorphic vision hybrid rram-cmos architecture,” *IEEE Transactions on Very Large Scale Integration (VLSI) Systems*, vol. 26, no. 12, pp. 2816–2829, 2018.
- [16] X. Zhang, W. Wang, Q. Liu, X. Zhao, J. Wei, R. Cao, Z. Yao, X. Zhu, F. Zhang, H. Lv *et al.*, “An artificial neuron based on a threshold switching memristor,” *IEEE Electron Device Letters*, vol. 39, no. 2, pp. 308–311, 2017.
- [17] Y. Zhang, Z. Wang, J. Zhu, Y. Yang, M. Rao, W. Song, Y. Zhuo, X. Zhang, M. Cui, L. Shen *et al.*, “Brain-inspired computing with memristors: Challenges in devices, circuits, and systems,” *Applied Physics Reviews*, vol. 7, no. 1, p. 011308, 2020.
- [18] Z. Wang, S. Joshi, S. Savel’ev, W. Song, R. Midya, Y. Li, M. Rao, P. Yan, S. Asapu, Y. Zhuo *et al.*, “Fully memristive neural networks for pattern classification with unsupervised learning,” *Nature Electronics*, vol. 1, no. 2, pp. 137–145, 2018.
- [19] F. Kiani, J. Yin, Z. Wang, J. J. Yang, and Q. Xia, “A fully hardware-based memristive multilayer neural network,” *Science advances*, vol. 7, no. 48, p. eabj4801, 2021.
- [20] E. O. Neftci, H. Mostafa, and F. Zenke, “Surrogate gradient learning in spiking neural networks: Bringing the power of gradient-based optimization to spiking neural networks,” *IEEE Signal Processing Magazine*, vol. 36, no. 6, pp. 51–63, 2019.

- [21] S. M. Kang, D. Choi, J. K. Eshraghian, P. Zhou, J. Kim, B.-S. Kong, X. Zhu, A. S. Demirkol, A. Ascoli, R. Tetzlaff, and L. O. Chua, "How to build a memristive integrate-and-fire model for spiking neuronal signal generation," *IEEE Transactions on Circuits and Systems I: Regular Papers*, 2021.
- [22] Y. LeCun, L. Bottou, Y. Bengio, and P. Haffner, "Gradient-based learning applied to document recognition," *Proceedings of the IEEE*, vol. 86, no. 11, pp. 2278–2324, 1998.
- [23] D. P. Kingma and J. Ba, "Adam: A method for stochastic optimization," *arXiv preprint arXiv:1412.6980*, 2014.
- [24] Q. Duan, Z. Jing, X. Zou, Y. Wang, K. Yang, T. Zhang, S. Wu, R. Huang, and Y. Yang, "Spiking neurons with spatiotemporal dynamics and gain modulation for monolithically integrated memristive neural networks," *Nature communications*, vol. 11, no. 1, pp. 1–13, 2020.
- [25] C. D. Schuman, T. E. Potok, R. M. Patton, J. D. Birdwell, M. E. Dean, G. S. Rose, and J. S. Plank, "A survey of neuromorphic computing and neural networks in hardware," *arXiv preprint arXiv:1705.06963*, 2017.
- [26] W. Wang, W. Song, P. Yao, Y. Li, J. Van Nostrand, Q. Qiu, D. Ielmini, and J. J. Yang, "Integration and co-design of memristive devices and algorithms for artificial intelligence," *Isience*, p. 101809, 2020.
- [27] L. A. Camuñas-Mesa, B. Linares-Barranco, and T. Serrano-Gotarredona, "Neuromorphic spiking neural networks and their memristor-cmos hardware implementations," *Materials*, vol. 12, no. 17, p. 2745, 2019.